

[G006]

**Markovian chemicals “in silico” design (MARCH-INSIDE), a promising approach for computer-aided molecular design III: 2.5D indices for the discovery of antibacterials.**

Humberto González-Díaz<sup>a,c,\*</sup>, Maykel Cruz-Monteagudo<sup>b</sup>, Luis A. Torres-Gómez<sup>c</sup>, Yaima Guevara<sup>c</sup>, Manuel S. Almeida<sup>d,e</sup>, Reinaldo Molina<sup>c,e</sup>, Nilo Castañedo<sup>c</sup>, Lourdes Santana<sup>a</sup>.

<sup>a</sup> *Department of Organic Chemistry, Faculty of Pharmacy, University of Santiago de Compostela, 15782, Spain.*

<sup>b</sup> *Applied Chemistry Research Center, Central University of Las Villas, 54830, Cuba.*

<sup>c</sup> *Chemical Bioactives Center, Central University of Las Villas, 54830, Cuba.*

<sup>d</sup> *Department of Chemistry, University of Granma, Cuba.*

<sup>e</sup> *Universität Rostock, FB Chemie, Albert-Einstein-Str. 3a, D 18059 Rostock, Germany.*

**Abstract** The present work continues our series on the use of MARCH-INSIDE molecular descriptors [parts I and II: *J. Mol. Mod.* (2002) 8: 237-245 and (2003) 9: 395-407]. These descriptors encode information regarding to the distribution of electrons in the molecule based on a simple stochastic approach to the idea of electronegativity equalization (Sanderson's principle). Here, 3D-MARCH-INSIDE molecular descriptors for 667 organic compounds are used as input for a Linear Discriminant Analysis. This 2.5D-QSAR model discriminates between antibacterial compounds and non-antibacterial ones with a 92.9 % of accuracy in training sets. On the other hand, the model classifies correctly 94.0 % of the compounds in test set. Additionally, the present QSAR performs similar-to-better than other methods reported elsewhere. Finally, the discovery of a novel compound illustrates the use of the method. This compound, 2-bromo-3-(furan-2-yl)-3-oxo-propionamide have MIC<sub>50</sub> of 6.25 and 12.50 µg/mL against *Ps. Aeruginosa* ATCC 27853 and *E. Coli* ATCC 27853 respectively while ampicillim, amoxicillim, clindamycin, and metronidazole have, for instance, MIC<sub>50</sub> values higher 250 µg/mL against *E. Coli*. Consequently, the present method may becomes a useful tool for the *in silico* discovery of antibacterials.

**Key Words:** Antibacterials, 3D-QSAR, Electronegativity Equalization, Markov Chains, Discriminant analysis.

\*Corresponding author Tel: +53/42/281473; Fax:+53/42/281130

E-mail: [humbertogd@vodafone.es](mailto:humbertogd@vodafone.es) or [humbertogd@uclv.edu.cu](mailto:humbertogd@uclv.edu.cu)

## Introduction

Quantitative-Structure-Activity Relationships (QSAR) methods have emerged due to the interest in finding efficient methods for the discovery of new drug-like compounds, understanding biological mechanism of action, and the search for compounds with the required profile of activity [1]. This method is based on the representation of molecular structure by certain numbers, the so-called molecular descriptors which are thereafter connected with biological activity by regression techniques [2, 3].

Quantum chemical calculations can be used to obtain a priori descriptors for QSAR studies. Given the fact that, some of these quantum properties are not observable, the way to calculate

them is not uniquely defined. Consequently, it is likely that there are many different schemes for their calculation, none of which is fundamentally more correct than other. Unfortunately, the computation is often also computationally too demanding for large sets of molecules [4]. In order to tackle this difficulty, Bultinck et al., described an implementation of a computational approach based on the Electronegativity Equalization Principle (EEP) to allow very fast calculation of atomic charges and related molecular descriptors [5]. According to EEP described by Sanderson, when molecules are formed, the electronegativities of the constituent atoms become equal coinciding with a fixed distribution for probabilities of finding the electrons in the neighbourhood of a specific atom in the molecule at the steady state [6-9]. Simpler and faster methods calculate molecular descriptors based on the idea of EEP are of interest for very large data bases of compounds to find drug-like leads.

Consequently, our research group has introduced a Markov chain (MC) approach based on the idea of EEP [10-19]. As a consequence, we were able to derive new molecular descriptors encoding the distribution of electrons in the molecule. The approach termed as **Markovian-Chemicals-In silico-Design (MARCH-INSIDE)** has shown to be very useful in drug design, toxicology, proteomics, and bioinformatics [10-19]. MARCH-INSIDE presents also interesting skills to codify 3D structural features such chirality and Z-E isomerism [12, 13, 19].

This last feature encourages us to study highly 3D-structure-dependent pharmacological activities like antibacterial action [20]. As a result of the widespread use of antibacterials has been rising the emergence of antibacterials-resistant pathogens, which in turn has fuelled an ever-increasing need for new drugs [21]. 2.5D-MARCH-INSIDE and Linear Discriminant Analysis (LDA) have been used to develop a QSAR in order to classify compounds as anti-bacterial or not, within structurally heterogeneous series, is presented in this work. The predictability for test set and comparison with respect to previously models validate this QSAR. In addition, the selection by virtual screening, synthesis, characterization, and preliminary assay of a novel compound illustrates how to use the model in practice. Finally, backprojection analysis of some compounds exemplifies the uses of the model for structure-activity relationships mapping.

## Materials and Methods

### *The basis of the 3D-MARCH-INSIDE approach*

The basis of the present approach has been explained in detail elsewhere [11]. Briefly, the model constitutes a stochastic approach to EEP. Consider a hypothetical situation in which a series of atoms interact to form a molecule at an arbitrary initial time ( $t_0$ ) [10-13, 18, 19]. Assume that after this initial situation, electrons start to distribute around atom cores in discrete intervals of time  $t_k$ . As depicted in **Figure 1**, this model describes the probabilities ( ${}^k p_{ij}$ ) with which electrons move from any arbitrary atom  $a_i$  at time  $t_0$  (in black) to other  $a_j$  atoms (in white) throughout discrete time periods  $t_k$  ( $k=1, 2, 3, \dots$ ) and throughout the chemical bonds.

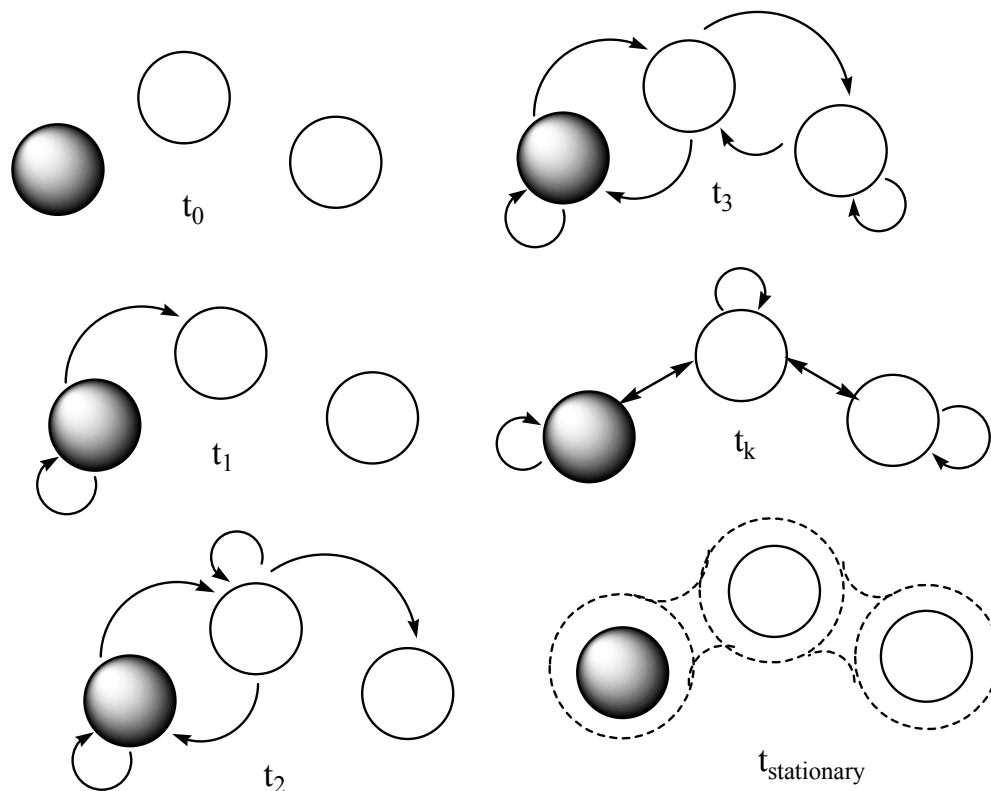


**Figure 1.** Diagrammatic representation a Markov model for electrons distribution. The symbol  $t_{\text{stationary}}$  represent the stationary time, electronegativity equalization.

The present procedure considers the external electron layers of any atom core in the molecule (valence shell) as states of the MC. The method uses the matrix  ${}^1\Pi$ , which has the elements  ${}^1p_{ij}$ . This matrix is called the 1-step electron-transition stochastic matrix.  ${}^1\Pi$  is built as a square table of order  $n$ , where  $n$  represents the number of atoms in the molecule. The elements ( ${}^1p_{ij}$ ) of the 1-step electron-transition stochastic matrix are the transition probabilities with which electrons move from atom  $i$  to  $j$  in the interval  $t_1 = 1$  (considering  $t_0 = 0$ ) [10-13, 18, 19]:

$${}^1p_{ij} = \frac{\chi_j \cdot e^{\omega_j}}{\sum_{k=1}^{\delta+1} \chi_k \cdot e^{\omega_k}} \quad (1)$$

Where,  $\chi_j$  is Pauling's electronegativity [22] for the atom  $a_j$ , which bounds to the atom  $a_i$ . In this equation  $\delta$  is the number of atoms which compete with  $a_i$  by its own electrons (atoms bound to  $a_i$ ) the number 1 account for the atom  $a_i$  *per se*. We will only use  ${}^1\Pi$  afterwards. The spatial configuration of every atom has been codified throughout the dummy variable  $\omega_j$ . This variable ( $\omega_j$ ) takes the value  $\omega_j = 1$  if the atom  $a_j$  is R, E or *axial* and the values  $\omega_j = 0, -1$  whether the atom  $a_j$  have not specific spatial configuration or present S, Z or *equatorial* configuration. The symbols R, S refers to the chirality of the atom. Alternatively, Z-E regards to the 3D characteristic for atoms involved in double bonds [12, 13, 19, 20]. The first step on calculating  ${}^1\Pi$  may be deriving an electronegativity matrix  $\chi$  which elements are isomer-indicator exponential functions coinciding with the numerators of expression like (1) [12, 13, 19]. In the short-term scale of time ( $t_1 = 1$ ) the movement of electrons is described here by  ${}^1\Pi$ , whilst the

probabilities of long-term movements are the elements of  ${}^k\Pi$ , ( $t_k = k > 0$ ) described herein by the Chapman–Kolmogorov equations [10-13, 23]:

$${}^k\Pi = ({}^1\Pi)^k \quad (2)$$

The method uses the sum of the self-return probabilities of the natural power of this matrix ( ${}^{SR}\pi_k$ ) as molecular descriptors. In classical Markov theory, these numbers are the probabilities with which the system returns to the initial state. In the present context, they are the probabilities with which electrons return to the original atoms at different times. That is to say, these numbers encode the distribution of electrons after the formation of the molecule as governed by EEP [10-13]. The calculation of  ${}^{SR}\pi_k$  for any organic or inorganic molecule was carried out using the MARCH-INSIDE software, being Tr the trace operator [24]:

$${}^{SR}\pi_k(\omega) = \sum_{i=1}^g {}^k p_{ii} = \text{Tr}({}^1\Pi^k) \quad (3)$$

### *Statistical Analysis*

In order to discriminate the antibacterial activity of drugs we will use a simple linear QSAR using 3D-MARCH-INSIDE with the general form:

$$A = b + b_0 \times {}^{SR}\pi_0(\omega) + b_1 \times {}^{SR}\pi_1(\omega) + b_2 \times {}^{SR}\pi_2(\omega) + \dots + b_k \times {}^{SR}\pi_k(\omega) \quad (4)$$

Here,  $b_k$  are the discriminant function coefficients fitted by Linear Discriminant Analysis. The model deals with the discrimination of antibacterial chemicals from non-active ones.

Examination of Fisher ratio (F) and the p-level (p) determines the quality of the model. We also inspect the percentage of good classification and the proportion between the cases and variables in the equation or variables to be explored in order to avoid over-fitting or chance correlation. Finally, predictability in an external prediction set validates the model; those compounds were never used to develop the classification function [25-27]. The ROC curves, and the area under these curves, were additionally used to validate the model [28].

Each compound was scored in terms of posterior probability by means of the posterior probability with which the compounds is classified as anticancer (P). This value constitutes a direct output of the model. This is a rigorous statistical index, which permits us to quote for the error. It possible to classify as antibacterial those compounds with  $P\% > 5$ , as a consequence that the model p-level threshold limit is 0.05. Conversely, those chemicals with  $P\% < -5$  must be classified as inactive ones. Whereas, chemicals in the range  $5 > P\% > 0$  must be considered as unclassified by the model at this p-level [10, 11].

### *Biological activity data used to seek the QSAR*

Here we considered a general data set composed by structurally diverse organic chemicals. This original set was split at random in order to design two different sets of antibacterial chemicals and two additional sets of non-antibacterial ones. Both antibacterial activity and chemical structure of each compound were verified in different references [29, 30]. For training, and predicting sets were considered as active those compounds recognized as antibacterials in the referred databases without taking into consideration the strain or the concentration of drug

required. Conversely such compounds having no effect against any strain were considered as non-active, as usual practice in all the QSARs reviewed below in Table 3.

### *Synthesis and Characterization*

Reagents were used as purchased without further purification. Solvents ( $\text{CHCl}_3$ ) were dried and freshly distilled before use according to literature procedures. Chromatographic TLC was performed on pre-coated silica gel polyester plates (0.25 mm thickness) with fluorescent indicator UV 254 (Polychrom SI F254). Melting point was determined on a Buchi 510 apparatus and is uncorrected. The IR spectrum was recorded on a Perkin-Elmer 1640FT spectrometer (KBr disk,  $\nu$  in  $\text{cm}^{-1}$ ). The  $^1\text{H-NMR}$  and  $^{13}\text{C-NMR}$  spectra were recorded on a Bruker WP 200-SY spectrometer at 200 MHz or on a Bruker SY spectrometer (400 MHz), the chemical shifts ( $\sigma$ ) are given in ppm downfield from tetramethylsilane. For EIMS analysis, a VG-TS250 apparatus (70 eV) was used. Elemental analysis was performed on a Perkin-Elmer 240B microanalyser and the values were within  $\pm 0.4\%$  of calculated ones in all cases.

#### **2-Bromo-3-(furan-2-yl)-3-oxo-propionamide:**

To a solution of 2-furoylacetonitrile (2.7 g, 0.02 mol) in chloroform (20 mL), was added under strong stirring anhydrous benzoyl peroxide (4.84 g, 0.02 mol). Thereafter, bromine (3.2 g, 0.02 mol) was added and the mixture was stirred for 2 h. at r. t. The solution was washed with water and  $\text{NaHCO}_3$  5%, dried over  $\text{Na}_2\text{SO}_4$  and the solvent was evaporated under vacuum. The solid residue was recrystallized from ethanol to give pure the desired compound (3.6 g, 77 % yield).

- Mp (dec.) = 155.8-156.7 °C.
- $^1\text{H-NMR}$  (acetone- $d_6$ ),  $\delta$ : furanic protons [7.94 (m, 1H, H-5), 7.55 (m, 1H, H-3), 6.75 (m, 1H, H-4)], 7.0-7.75 (m, 2H exch.,  $\text{NH}_2$ ), 5.73 (s, 1H, CH).
- $^{13}\text{C-NMR}$  (acetone-  $d_6$ ),  $\delta$ : furanic carbons [150.82 (C-2), 149.25 (C-5), 120.92 (C-3), 113.7 (C-4)], 178.83 (C=O), 184.5 (C=O), 47.51 (CH).
- EIMS (70 eV)  $m/z$  (%): 231 ( $\text{M}^+$ ), 233 ( $[\text{M}+2]^+$ ), 152 (41), 95 (98), 31 (100).
- IR  $\nu$ : 3423, 3301, 1666, 1656.
- Anal.  $\text{C}_7\text{H}_6\text{BrNO}_3$ : C, H, N.

### *Biological Assay of a new compound*

This study was carried out with a new compound do not contained in the training or predicting series but predicted afterwards. *In vitro* Minimal inhibitory concentration ( $\text{MIC}_{50}$ ) assays were carrying out throughout the Mueller-Hinton serial dilution method according to recommendations of the National Committee for Clinical Laboratory Standards [31, 32]. The  $\text{MIC}_{50}$  value was determined for two ATCC reference bacterial strains: *Ps. aeruginosa* ATCC 27853 and *E. coli* ATCC 27853 were carried out.

## **Results and Discussion**

### *QSAR Modelling*

Once we split at random the original data in representative training and test set, the training set may be used to seek the discriminant function using LDA. The model selection was subjected to

the principle of parsimony or Occam's Razor [27]. As a result; we chose a function with higher statistical signification but with few parameters ( $b_k$ ) as possible:

$$A_{\text{stand}} = 0.02^{\text{SR}} \pi_0(\omega) + 1.57^{\text{SR}} \pi_2(\omega) - 3.56^{\text{SR}} \pi_3(\omega) + 4.33^{\text{SR}} \pi_4(\omega) \quad (5)$$

$$- 19.5^{\text{SR}} \pi_6(\omega) + 24.8^{\text{SR}} \pi_7(\omega) - 7.8^{\text{SR}} \pi_9(\omega) + 4.221$$

$$F = 139.27 \quad p < 0.001$$

Where,  $A_{\text{stand}}$  is a dummy variable (1 for antibacterial compounds and -1 for non-active ones). Prior to fitting all molecular descriptors were mean centred and normalized avoiding certain descriptors dominating the model. Fisher test allow us to test the hypothesis of separation of groups with a probability of error (p-level)  $p < 0.05$ . All the parameters have the same values for equations, 5 and 6 [10, 11, 27, 33].

The model correctly classifies 92.9 % of the compounds in the training set. Specifically, the model correctly classifies 252 out of 274 (91.9 %) antibacterial compounds and 205 out of 218 (93.9 %) inactive compounds in training set. In both stets, albeit the model is not strictly 3D the use of  $\omega$  allowed taking into consideration compounds with specific 3D structure. The names of all compounds used to derive the QSAR as well as their predicted activity appear in Table 1 (see supplementary material). Compounds were ordered according to different intervals of predicted activity.

On the other hand, prediction series shows a 94.0 % of global predictability. In this study the discriminant function has given rise for a good classification of 85 out of 92 (95.9 %) and 79 out of 83 (92.2 %) of non-active drugs respectively. The names of all compounds used to validate the QSAR as well as their predicted activities appear in Table 2, see supplementary information. Both, training and predicting sets percentages of good classification validates the model for the use in virtual screening taking into consideration that 85.0 % is considered as an acceptance threshold limit for this kind of analysis [34].

In any case, a more serious validation was carry out by calculating the areas under the receiver operating characteristic (ROC) curve to show how well the model classifies. The **Figure 2** depicts by separate the ROC curves obtained for compounds on training and predicting sets with area under curve of 0.98 and 0.97 respectively, a ROC area of 1.0 indicates perfect classification. It can be visually detected a clear difference between both ROC curves and the line in the main diagonal which represent a random classifier area under curve equal to 0.5 [28].

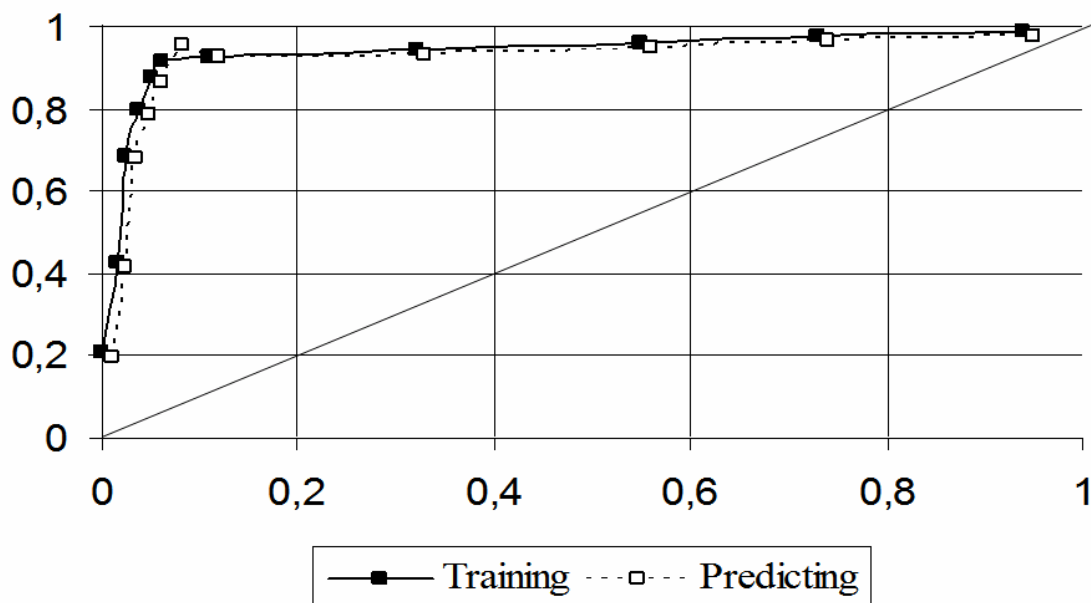


**Figure 2.** Operating Receive Characteristic curve (ROC-curve) for training and predicting series of antibacterial and non-active compounds.

#### *Comparison with other models*

The present QSAR performs better-to-similar with respect to other eleven models based on large heterogeneous series of antibacterial/non-antibacterial compounds too, see Table 3 on supplementary information material [35-41]. In addition to those ten models in the Table 3 another interesting work on antibacterial activity was developed by Mishra *et al.* [42]. However, the largest data studied by Mishra and co-workers incorporated only 463 compounds (242 antibacterials) with about 84% of overall predictability and do not involve 3D or 2.5D indices. Briefly, the present model has some interesting characteristics (see Table 3, salient points in boldface fonts):

1. Use the largest up-to-date reported data set of experimentally corroborated antibacterial compounds (363) for a QSAR study.
2. A broad range of applicability for this model can be stressed considering the larger number of families of different organic compounds used.
3. It must also be noted that on seeking the present model we explored only 10 molecular descriptors.
4. This model makes use by the first time of chiral topologic indices [43] for the search of antibacterial compounds.
5. The quality of the predictions of this model have been assessed using a more rigorous test set method namely, re-substitution. Some of the other models assessed predictability using cross validation methods (e.g. leave-one-out or jackknife).

Table 3. Comparison with other approaches.

Models' features to be compared <sup>a</sup>	Antibacterial activity classification models										
	1	2	3	4	5	6	7	8	9	10	11
N total	667	661	661	661	352	111	111	-	972	458	433
N antibacterials	<b>363</b>	249	249	249	174	60	60	-	241	229	217
Technique <sup>b</sup>	LDA	LDA	BLR	ANN	LDA	LDA	ANN	LDA	LDA	LDA	LDA
U-statistics (Wilk's $\lambda$ )	<b>0.38</b>	-	-	-	0.45	0.28	-	0.57	0.58	0.56	-
F	<b>139.3</b>	-	-	-	48.2	20.9	-	116.6	98	98	-
D <sup>2</sup>	5.33	-	-	-	4.9	-	-	-	-	-	-
p-level	0.00	-	-	-	0.00	0.00	-	0.00	0.00	0.00	0.00
3D-topologic indices <sup>c</sup>	<b>yes</b>	no	no	no	no	no	no	no	no	no	no
Explored variables	<b>10</b>	167	167	62	10	16	16	-	-	-	62
Vars. in model	7	6	6	62	7	7	7	8	8	2	6
Back-projection <sup>d</sup>	<b>yes</b>	no	no	no	yes	no	no	no	no	no	no
Training series											
N total	492	661	661	661	289	64	64	294	698	355	433
N antibacterials	<b>274</b>	249	249	249	174	34	34	-	169	161	217
Accuracy (%)	92.85	92.6	94.7	-	91	94.0	89.0	> 90	86.8	~ 85	~ 85
Families of drugs <sup>e</sup>	<b>11</b>	8	8	8	9	3	3	-	> 5	-	> 8
Validation											
Validation method <sup>f</sup>	i	ii	ii	iii	i	i	i	i	i	i	i
N total	175	-	-	63	63	47	47	70	274	103	128
N antibacterials	<b>89</b>	-	-	45	45	26	26	-	72	68	64
Predictability (%)	94	93.6	94.3	~ 94	89	92	97.9	> 90	86.9	~ 85	~ 85
Families of drugs <sup>b</sup>	<b>11</b>	-	-	8	9	3	3	-	> 5	-	> 8

<sup>a</sup> Model 1 is reported in this work, models 2 and 3 were reported by Cronin *et al.* in reference [35], model 4 appears in reference [36] after Tomás-Vert *et al.*, model 5 was very recently reported by Molina E. *et al.* (reference [37]), models 6 and 7 were published in 1998 (reference [38]), model 8 was developed by Mut-Ronda *et al.*, [39], two LDA models were recently introduced by Murcia-Soler *et al.*; model 9 in [39] and 10 in reference [41]. The last model here depicted was published by Gregorio-Alapont *et al.* [42].

<sup>b</sup> LDA refers to Linear discriminant analysis, ANN to artificial neural network, and BLR to binary logistic regression.

<sup>c</sup> Considers the capability of the method to encode together chirality, Z-E, and axial-equatorial isomerism.

<sup>d</sup> Considers the possibility of deriving a map with the calculated contribution of any atom in the molecule to the biological activity.

<sup>e</sup> Only largely represented families were considered, e. g. methods 1 and 2 used 3 in training quinolones, sulphonamides, and cephalosporins but add only diaminopyridine (1 compound), cephamicins (2), oxacephems (1) and sulfones (1) to predicting series.

<sup>f</sup> Validation methods are: i) external predicting series, ii) leave-30%-out crossvalidation, and iii) 100-times-averaged re-substitution technique. Furthermore, note that methods ii and iii are cross-validation methods.



The previous topologic models do not consider 3D structure, although the present model does not consider geometric 3D information may discriminate drugs with different 3D structure due to the use of  $\omega$ , including optic and Z-E isomers. Consequently, predictions using the former models are expected to fail in such very commonly occurring cases in which stereochemistry determines the biological activity [12, 18, 19, 20, 44]. The discrimination of different kinds of stereo-isomers has been fully exemplified before for 3D-MARCH-INSIDE [12, 13, 19] and, **Figure 3** illustrates this aspect for a simple example. It is straightforward to realise that, the more different the matrices are for a pair of isomers the larger the differences for its calculated molecular descriptors. We would like highlighting that the present comparison does not involve the skills of different indices as molecular descriptors. In fact, recent results report the generalization of classic connectivity indices for chirality codification [43-46]. The present comparison refers only to the range of applicability of the reported QSARs with respect to the present one.

[R]-CHClBrF						[S]-CHClBrF					
$\chi_{ij}$	H	F	C	Br	Cl	$\chi_{ij}$	H	F	C	Br	Cl
H	2.1	0	6.8	0	0	H	2.1	0	0.92	0	0
F	0	4	6.8	0	0	F	0	4	0.92	0	0
C	2.1	4	6.8	2.8	3	C	2.1	4	0.92	2.8	3
Br	0	0	6.8	2.8	0	Br	0	0	0.92	2.8	0
Cl	0	0	6.8	0	3	Cl	0	0	0.92	0	3
${}^1\Pi(R)$						${}^1\Pi(S)$					
	H	F	C	Br	Cl		H	F	C	Br	Cl
H	0.24	0	0.76	0	0	H	0.7	0	0.3	0	0
F	0	0.4	0.63	0	0	F	0	0.8	0.19	0	0
C	0.11	0.2	0.36	0.15	0.16	C	0.16	0.3	0.07	0.22	0.23
Br	0	0	0.71	0.29	0	Br	0	0	0.25	0.75	0
Cl	0	0	0.69	0	0.31	Cl	0	0	0.23	0	0.77
${}^2\Pi(R)$						${}^2\Pi(S)$					
	H	F	C	Br	Cl		H	F	C	Br	Cl
H	0.14	0.2	0.46	0.11	0.12	H	0.53	0.1	0.23	0.07	0.07
F	0.09	0.4	0.25	0.12	0.13	F	0.03	0.6	0.35	0.04	0.04
C	0.1	0.2	0.35	0.15	0.16	C	0.09	0.2	0.43	0.13	0.14
Br	0.1	0.2	0.26	0.29	0.15	Br	0.04	0.1	0.4	0.45	0.05
Cl	0.1	0.2	0.26	0.13	0.31	Cl	0.03	0.1	0.39	0.05	0.47

**Figure 3.** Depicts the different electronegativity matrix  $\chi$  (which elements are equal to  $\chi_{ij} \cdot \exp(\omega_{ij})$ ) if atom  $a_i$  bounds to atom  $a_j$  or equal to 0 otherwise, the normalized stochastic or Markov matrix  ${}^1\Pi$  derived from  $\chi$  and its first power  ${}^2\Pi$  for a pair of mirror isomers.

### Virtual Screening

Finally, the discovery of 2-bromo-3-(furan-2-yl)-3-oxo-propionamide as a novel antibacterial compound illustrates the use of the model in practice. First, the  ${}^{SR}\pi_k(\omega)$  values were calculated for a large data set of organic compounds. Unfortunately, the whole data it is not available for the moment due to ongoing patenting process. Anyhow, this data it is not necessary to reproduce the present work taking into consideration that only training and validation sets have to be used

in doing so. Secondly, the posterior probabilities of antibacterial activity are predicted with the 3D-QSAR. Last, the compound with the highest probabilities was synthesized starting from the 2-furoylacetonitrile, with yield of 77.0 % (**Figure 4**).

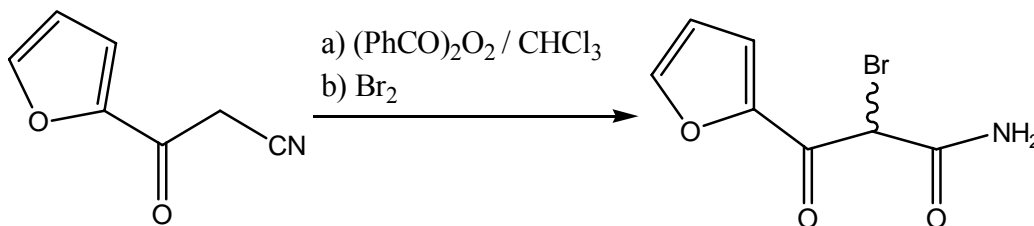


**Figure 4.** Synthesis of 2-bromo-3-(fur-2-yl)-3-oxo-propionamide.

After biological assay this amide showed MIC<sub>50</sub> values of 6.25 and 12.50 µg/mL against *Ps. Aeruginosa* ATCC 27853 and *E. Coli* ATCC 27853 respectively, which constitute strains of bacterial species with a high clinical incidence. With these MIC<sub>50</sub> the compound may be considered useful as a lead compared for instance with MIC<sub>50</sub> for ceftriaxone, a commercial drug, which present a MIC<sub>50</sub> of 0.06 against µg/mL *E. Coli* but 64.0 µg/mL against *Ps. Aeruginosa* [47]. However, *E. Coli* has developed resistance against several broad spectrum antibacterial drugs such as ampicillim, amoxicillim, clindamycin, and metronidazole with MIC<sub>50</sub> values higher 250.0 µg/mL in all cases [48]. In the present case both enantiomers were predicted with similar high probabilities, so we decided do not separate them in this preliminary study. More rigorous studies aimed on the synthesis, characterization, stability, biological testing, and the mechanism of action (now unknown) of both enantiomers and their derivatives are in any case beyond of the scope of the present paper.

#### *Backprojection analysis*

Finally, to gain further insight into the role played by the different molecular features a back-projection approach was applied. Specifically, the use of back-projectable approaches enables the variables on the QSAR to be projected back into the molecular space, providing for biological and chemically significant conclusions. The MARCH-INSIDE descriptors introduced by our research group constitutes another example of novel back-projectable molecular descriptors. Specifically, the model introduced in the present work may be used to draw visual structure-activity maps for drugs in training and test set, as well as for the novel compound herein reported by the first time. This analysis makes it possible to calculate the contribution of the different groups of atoms in the molecule to the pharmacological activity. First, the <sup>SR</sup>π<sub>k</sub> values for each atom in the molecule are calculated and afterwards they are evaluated in the QSAR equation. All values are normalized within 0 to 100 scales [49].

Figure 5 depicts these maps for Nitrofurantoin, Cefuroxime, Nifuroxime, and 2-bromo-3-(fur-2-yl)-3-oxo-propionamide. Interestingly, one can note that the furan ring presented high positive contributions to the activity in Nitrofurantoin, and Nifuroxime, which are 5-nitro-furans with a double bond (C=N) attached to position 2 of the furan ring. These classes of compounds are

expected to bind the target by nucleophilic substitution at the double bond activated by the electron-withdrawing Nitro group. In this sense, our maps coincide with previous knowledge. Conversely, in Cefuroxime the highest contribution was calculated for the  $\beta$ -lactamic framework with not significant contribution of the furan ring. This fact coincides with the structure-activity relationships for cephalosporin. In the case of 2-bromo-3-(fur-2-yl)-3-oxo-propionamide a high contribution for the furan ring it is predicted too, it indicates that this compounds is more likely to nitro-furans [21].

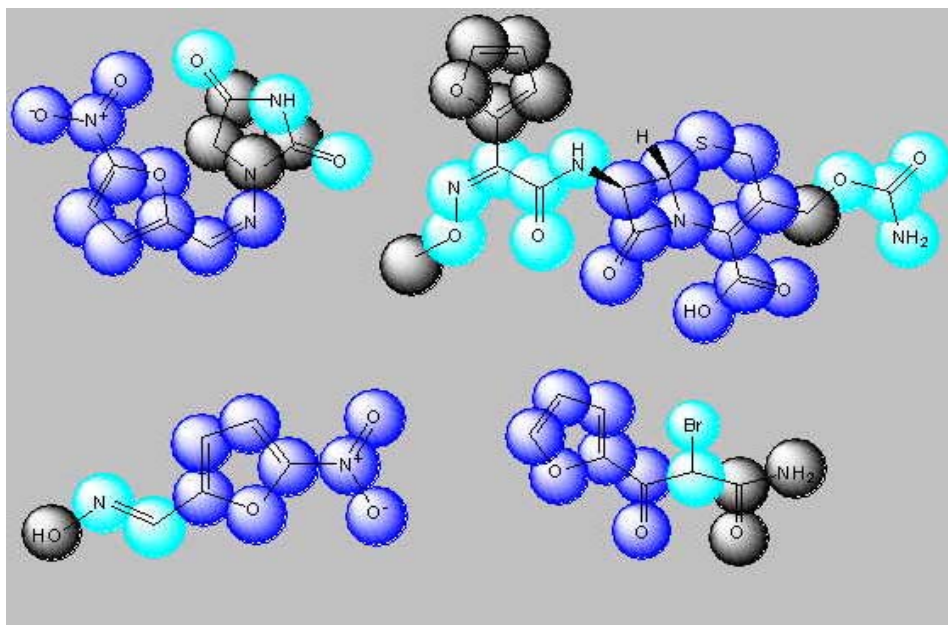


**Figure 5.** Colour scaled backprojection analysis of some compounds in training and predicting sets: Nitrofurantoin (left top), Cefuroxime (right top), Nifuroxime (left bottom) and 2-bromo-3-(fur-2-yl)-3-oxo-propionamide (right bottom). Colour code is as follows: Blue: structural framework with high (more than 50 %) contribution to the property, Light blue: group with significant contribution (20-50 %), Grey: group with low (< 10 %) or not contribution to the property.

The explosion in the use of novel topologic molecular descriptors will continue in the future. The fusion of High Throughput Screening with QSAR techniques is a new promising field [50]. In conclusion, the aforementioned modelling results introduce a timely way for the discovery of antibacterial lead like compounds taking into consideration 3D structural features.

### Supplementary material

Enclosed supplementary material depicts the names and posterior probabilities of all compounds in train (Table 1) and prediction sets (Table 2).

### Acknowledgements

We thank the Spanish Ministry of Science and Technology (SAF2003-02222), for partial financial support. Molina RR, Castañedo C, and Almeida SM, acknowledges support from the

Universität Rostock, Germany. Both unknown referees are acknowledged by their useful comments.

## References

1. Randić M, Sabljčić A, Nikolić S, Trinajstić N (1988) *Int. J. Quantum Chem. Quantum Biol. Symp.* 15: 267-285.
2. Kier LB, Hall LH (1999) *Topological indices and related descriptors in QSAR and QSPR*. Gordon and Breach, Amsterdam, pp 455–489.
3. Todeschini R, Consonni V (2000) *Handbook of molecular descriptors*. Mannhold, R, Kubinyi, H, Timmermann, H, Ed., Wiley-VCH: Weinheim.
4. Karelson M, Lobanov VS, Katritzky AR (1996) *Chem. Rev.* 96: 1027-1043.
5. Bultinck P, Langenaeker W, Carbó-Dorca R, Tollenaere JP (2003) *J. Chem. Inf. Comput. Sci.* 43: 422-428.
6. Sanderson RT (1951) *Science* 114: 670.
7. Sanderson RT (1983) *Polar covalence*. Academic Press, New York.
8. Gasteiger J, Marsili M (1980) *Tetrahedron* 36: 3219-3228.
9. Mortier WJ, Gosh SK, Shankar S (1986) *J. Am. Chem. Soc.* 108: 4315-4320.
10. González-Díaz H, Olazábal E, Castañedo N, Hernández S. I, Morales A, Serrano H. S, González J, Ramos de A. R (2002) *J. Mol. Mod.* 8: 237-245.
11. González-Díaz H, Gia O, Uriarte E, Hernández SI, Ramos de A. R, Chaviano M, Seijo S, Castillo JA, Morales L, Santana L, Akpaloo D, Molina E, Cruz M, Torres L. A, and Cabrera MA (2003) *J. Mol. Mod.* 9: 395-407.
12. González-Díaz H, Bastida I, Castañedo N, Nasco O, Olazábal E, Morales A, Serrano SS, Ramos de AR *Bull. Math. Biol.* (2004) doi: 10.1016/j.bulm.2003.12.003.
13. González-Díaz H, Marrero, Y, Hernández SI, Bastida I, Tenorio I, Nasco O, Uriarte E, Castañedo N, Cabrera M, Aguila E, Marrero O, Morales A, and Pérez M. (2003) *Chem. Res. Toxicol.* 16: 1318-1327.
14. González-Díaz H, Ramos de AR, Uriarte E (2002) *Online J. Bioinf.* 1: 83-95.
15. González-Díaz H, Ramos de AR, Molina RR (2003) *Bull. Math. Biol.* 65: 991-1002.
16. González-Díaz H, Ramos de AR, Molina RR (2003) *Bioinformatics* 19: 2079-2087.
17. González-Díaz H, Molina RR, Uriarte E (2004) *Polymer* 45: 3845–3853.
18. Ramos de AR, González-Díaz H, Molina RR, Uriarte E (2004) *Proteins: Struct. Funct. Bioinf.* doi: 10.1002/prot.20159.
19. González-Díaz H, Hernández SI, Uriarte E, Santana L (2003) *Comput. Biol. Chem.* 27: 217-227.
20. Eliel E, Wilen S, Mander L (1994) *Stereo Chemistry of Organic Compounds*, John Wiley & Sons Inc, New York. pp 103-112.
21. Hardman GJ, Lee EI (1996) *Goodman and Gilman's, The Pharmacological basis of Therapeutics*, 9th edition, McGraw-Hill.
22. Pauling L (1939) *The nature of chemical bond*, Cornell University Press, Ithaca, New York, pp 2-60.
23. Freund JA, Poschel T (2000) *Stochastic Processes in Physics, Chemistry, and Biology*. In: *Lect. Notes Phys.* Springer-Verlag, Berlin, Germany.
24. González-Díaz H, Molina RR, Hernández SI (2003) **MARCH-INSIDE 2.0** ® (**Markovian Chemicals "In Silico" Design**) Chemical Bioactives Center, Central

University of “Las Villas”, Cuba. The present constitutes a preliminary experimental version; future professional versions shall be available to the public free of charge. For any information about it, sends and e-mail to the corresponding author: [humbertogd@vodafone.es](mailto:humbertogd@vodafone.es) or [humbertogd@cbq.uclv.edu.cu](mailto:humbertogd@cbq.uclv.edu.cu).

25. Kowalski RB, Wold S (1982) Pattern recognition in chemistry, In: Handbook of statistics. Eds: Krishnaiah PR, Kanal LN. North Holland Publishing Company, Amsterdam. pp 673-697.
26. STATISTICA (2002) Statsoft, Inc. version. 6.0.
27. Van Waterbeemd H (1995) Discriminant analysis for activity prediction, in: Method and Principles in Medicinal Chemistry. Chemometric methods in molecular design, VCH, Weinhiem. pp 265-282.
28. Swets JA (1988) Science 240: 1285-93.
29. Kleeman A, Engel J, Kutscher B, Reichert D (2001) Pharmaceutical Substances 4th, George Thieme Verlag, Stuttgart.
30. Negwer M (1987) Organic chemical drugs and their synonyms, Akademie-Verlag, Berlin.
31. The ATCC Bacteriology Collection (2002):  
<http://www.atcc.org/SearchCatalogs/Bacteria.cfm>
32. National Committee for Clinical Laboratory Standards (2000) Methods for dilution antimicrobial susceptibility tests for bacteria that grow aerobically. Approved standard M7-A5. Wyne, Pa.
33. González MP, González-Díaz H, Molina RR, Cabrera MA, Ramos de AR (2003) J. Chem. Inf. Comput. Sci. 43: 1192-1199.
34. Gálvez J, García R, Salabert MT, Soler R (1994) J Chem Inf Comput Sci 34: 520–525.
35. Cronin MTD, Aynur AO, Dearden CJ, Deffy CJ, Netzeva IT, Patel H, Rowe HP, Schultz TW, Worth PA, Voutzolidis K, Schüürmann G (2002) J. Chem. Inf. Comput. Sci. 42: 869-878.
36. Tomás-Vert F, Pérez-Giménez F, Salabert-Salvador MaT, García-March FJ, Jaén-Oltra J (2000) J. Mol. Struct. Theochem. 504: 249-259.
37. Molina E, González-Díaz H, González MP, Rodríguez E, Uriarte E. (2004) J. Chem. Inf. Comput. Sci. 44: 515-521.
38. García-Domenech R, Julián-Ortiz JV (1998) J. Chem. Inf. Comput. Sci. 38: 445-449.
39. Mut-Ronda S., Salabert-Salvador MT, Duart MJ, Antón-Fos GM (2003) Bioorg. Med. Chem. Lett. 13: 2699-2702.
40. Murcia-Soler M, Pérez-Giménez F, García-March FJ, Salabert-Salvador MT, Díaz-Villanueva W, Medina-Casamayor P. J. Mol. Graph. Mod. (2003) 21: 375-390.
41. Murcia-Soler M, Pérez-Giménez F, García-March FJ, Salabert-Salvador MT, Díaz-Villanueva W, Castro-Bleda MJ, Villanueva-Pareja A. J. Chem. Inf. Comput. Sci. (2004) 44: 1031 – 1041.
42. Mishra RK, Garcia-Domenech R, Galvez J (2001) J. Chem. Inf. Comput. Sci. 41: 383-393.
43. Golbraik A, Bonchev D, Tropsha A (2001) J. Chem. Inf. Comput. Sci. 41, 147.
44. Julián-Ortiz JV, de Gregorio Alapont C, Ríos-Santamaria I, García-Domenech R, and Gálvez J (1988) J. Mol. Graphics Modell. 16: 14-18.
45. Kellogg GE, Kier LB, Gaillard P, Hall LH (1996) J. Comput.-Aided Mol. Des. 10: 513-520.

46. Golbraik A, Bonchev D, Tropsha A (2001) *J. Chem. Inf. Comput. Sci.* 41: 147-158.
47. Fujimura T, Yamano Y, Yoshida I, Shimada J, Kuwahara S (2003) *Antimicrob. Agents Chemoter.* 47: 923-931.
48. Handal T, Caugant DA, Olsen I (2003) *Antimicrob. Agents Chemoter.* 47: 1443-1446
49. Stilt, N.; Baumann, K. (2003) *J. Med. Chem.* 46, 1390-1407.
50. Devillers J, Balaban AT (2000) *Topological indices and related descriptors in QSAR and drug design.* Amsterdam, pp 3–41.